Polymer 49 (2008) 5322–5328

Contents lists available at ScienceDirect

Polymer

journal homepage: www.elsevier.com/locate/polymer

Double thermoresponsive polybetaine-based ABA triblock copolymers with capability to condense DNA

Fengying Dai [a], Pengfei Wang [a], Ying Wang [b], Lei Tang [a], Jianhai Yang [a], Wenguang Liu [a,*], Hexian Li [b], Guochang Wang [b]

[a] School of Materials Science and Engineering, Tianjin Key Laboratory of Composite and Functional Materials, Tianjin University, Tianjin 300072, PR China
[b] Key Laboratory of Functional Polymer Materials Ministry of Education, Nankai University, Tianjin 300071, PR China

ARTICLE INFO

Article history:
Received 8 July 2008
Received in revised form 9 September 2008
Accepted 30 September 2008
Available online 9 October 2008

Keywords:
Polysulfobetaine
2-(2-Methoxyethoxy)ethyl methacrylate
DNA complex

ABSTRACT

ABA type MPDSAH$_y$-*b*-PMEO$_2$MA$_x$-*b*-MPDSAH$_y$ (A = *N*-(3-(methacryloylamino)propyl)-*N*,*N*-dimethyl-*N*-(3-sulfopropyl) ammonium hydroxide (MPDSAH), B = 2-(2-methoxyethoxy)ethyl methacrylate (MEO$_2$MA)) triblock copolymers with narrow polydispersity index were prepared by atomic transfer radical polymerization (ATRP) in the mixture of water/methanol with addition of sodium chloride. The copolymer solution was shown to exhibit UCST and LCST behaviors. The dual temperature sensitiveness was investigated via turbidity measurement and steady-state fluorescence spectroscopy. The UCST was found to be dependent upon the solution concentration, and UCST shifted towards LCST with the increment in the block length of MPDSAH block. In the selected low temperature region, the micropolarity of pyrene slightly increased due to the weak positive–negative interaction in diluted solution; while above LCST, pyrene experienced more hydrophobic milieu owing to the noticeable dehydration of PMEO$_2$MA. The analysis of ethidium bromide displacement suggested the strong capability of MPDSAH homopolymer to bind DNA; MEO$_2$MA moieties in copolymers weakened the binding ability of PMPDSAH to DNA, but 54–60% EB was still replaced by copolymers at complexing ratio of 10/1. AFM confirmed that PMPDSAH and copolymers were capable of condensing DNA to nanoparticles at an appropriate complexing ratio. Complexing with DNA, UCST of solution vanished, but LCST was slightly increased due to the enhanced hydrophilicity caused by liberation of negative charges.

1. Introduction

Polybetaines (PBs, sulfo-, phospho-, and carboxybetaine) bearing both anionic and cationic groups on the same monomer units are one type of very interesting polyelectrolytes, and not only have aroused increasing academic attention due to their unique polyelectrolyte properties [1,2], but also found wide applications in diverse fields such as water treatment, cosmetics, drag reduction and pharmaceuticals [3–7]. Among the synthetic PBs currently available, polysulfobetaine was shown to exhibit upper critical solution temperature in aqueous solution, good blood compatibility and nonfouling property [8–12]. To date, more studies were concerned with sulfobetaine-based statistical copolymers prepared by random free radical polymerization, which lacked well-defined molecular architecture [1,13,14]. In their earlier work, Armes et al. [14] used GTP to synthesize narrow disperse poly(2-(dimethylamino)ethyl methacrylate) (PDMAEMA) precursor, which was then betainised to convert into polysulfobetaine. Jiang et al. [15] reported on the synthesis of poly(sulfobetaine methacrylate)-poly(propylene oxide) (polySBMA–PPO) diblock copolymers by sequential ATRP. The polydispersity index of polySBMA–PPO copolymer was controlled at 1.23–1.35. After the hydrophobic surface is back-filled with the copolymer of small molecular weight, protein adsorption was highly resisted.

Recently, schizophrenic poly(*N*-isopropylacrylamide)-*b*-poly(3-[*N*-(3-methacrylamidopropyl)-*N*,*N*-dimethyl] ammoniopropane sulfonate) block copolymer (PNIPAAm–PSPP) was synthesized by Laschewsky via RAFT [16]. The PNIPAAm–PSPP was found to display LCST and UCST behaviors in water. It was considered that the change in the polarity of micellar core in the process of reversible phase transition provided the possibility of solubilizing different compounds in a given solution just by simple heating and cooling. Despite the most popularity in thermorepsonsive polymers, the biosafety of PNIPAAm remains concern in the body [17]. More recently, Lutz et al developed temperature sensitive poly[2-(2-methoxyethoxy)ethyl methacrylate], poly[oligo(ethylene glycol) methacrylate] as well as their copolymers, which showed LCST behavior and were arguably a promising alternative to PNIPAAm

* Corresponding author. Tel./fax: +86 22 27402487.
E-mail address: wgliu@tju.edu.cn (W. Liu).

0032-3861/$ – see front matter © 2008 Elsevier Ltd. All rights reserved.
doi:10.1016/j.polymer.2008.09.060

in view of the fairly high biocompatibility and superior temperature sensitiveness [18–22].

By the above literature retrospection, we thought it would be very interesting to construct copolymers based on two biocompatible components of polysulfobetaine and temperature sensitive PEG analog. However, so far, there has been no such research work in literature as far as we are concerned. Thus, we are motivated to synthesize ABA type PMPDSAH/$PMEO_2MA$ triblock copolymers by ATRP in this study. We will examine the dual thermoresponsive behaviors of PMPDSAH/$PMEO_2MA$ copolymer in aqueous solution. In addition, the interpolyelectrolyte interaction between PMPDSAH/$PMEO_2MA$ with DNA will also be explored. Traditionally, in developing non-viral vector for gene delivery, DNA was condensed by polyelectrolyte, but the charge neutralization tended to cause precipitate of complex, restricting the stability of storage and transport in blood. In our work, PMPDSAH is a polyzwitterion in which the quaternary ammonium cations contribute to the condensation of DNA; while its partner sulfonic anions remain unreacted, thus providing the shielding of inter-complex coacervation. That will be of great significance in construction of novel gene delivery system. In this study, the effect of DNA on UCST and LCST of copolymer solution will be studied as well.

2. Experimental part

2.1. Materials

2-(2-Methoxyethoxy)ethyl methacrylate (MEO_2MA, 95%), *N*,*N*,*N*′,*N*′,*N*″-pentamethyldiethylenetriamine (PMDETA, 99%), *N*-(3-(methacrylamido)propyl)-*N*,*N*-dimethyl-*N*-(3-sulfopropyl) ammonium hydroxide (MPDSAH, 97%), copper(I) chloride (CuCl), diethyl-meso-2,5-dibromoadipate (DEDBA) were purchased from Aldrich Chemical Co. and used without further purification. Ethidium bromide (EB) was supplied by Fluka. Calf thymus DNA (5000 bp, Sigma Chemical Co.) was used in EB replacement and turbidity measurement. Plasmid DNA (5256 bp, Promega Co.) was used in AFM measurement. All other reagents used were of analytical grade.

2.2. Synthesis of $MPDSAH_y$–MEO_2MA_x–$MPDSAH_y$ copolymers

The two-step synthetic route of ABA type $MPDSAH_y$–MEO_2MA_x–$MPDSAH_y$ triblock copolymer was depicted in Scheme 1.

In a typical run, DEDBA (4.3 mg, 0.012 mmol) and Cu(I)Cl (2.4 mg, 0.024 mmol) dissolved in 2 ml methanol were placed into a Schlenk tube and degassed via three freeze–thaw cycles. MEO_2MA (0.23 g, 1.2 mmol, target degree of polymerization = 100) and PMDETA (4.2 mg, 0.024 mmol) dissolved in 6 ml methanol were then added via a syringe under nitrogen and the reaction mixture was degassed via another three freeze–thaw cycles. The reactor was placed in a thermostated oil bath at 60 °C. After 2 h, the reactor was cooled by liquid nitrogen to terminate the reaction. The catalyst was removed using a basic alumina column, and the polymer was recovered by precipitation in excess of *n*-hexane and dried under vacuum. The reprecipitation process was repeated three times to remove unreacted monomer and impurities.

MEO_2MA_{100} macro-initiator (0.12 g, 0.012 mmol), Cu(I)Cl (2.4 mg, 0.024 mmol) and 2 ml methanol were placed into a Schlenk tube and degassed via three freeze–thaw cycles. Degassed mixture MPDSAH (0.35 g, 1.2 mmol), NaCl (2.8 mg, 0.048 mmol) and PMEDTA (4.2 mg, 0.024 mmol) dissolved in 6 ml ultrapure water were then added under nitrogen. The reactor was placed at room temperature. After 2 h, the reactor was cooled by liquid nitrogen to terminate the reaction. Then the solvent was evaporated off, and the copolymer was dissolved in deionized water followed by dialysis in a Cellu SepH1-membrane (MWCO3000) to remove the impurities and unreacted monomers. Finally, the white triblock copolymer was collected by freeze-drying overnight. The resultant copolymer was denoted as $MPDSAH_{50}$–MEO_2MA_{100}–$MPDSAH_{50}$.

Similarly, copolymers of $MPDSAH_{20}$–MEO_2MA_{160}–$MPDSAH_{20}$, $MPDSAH_{80}$–MEO_2MA_{40}–$MPDSAH_{80}$ and $PMEO_2MA$ and PMADSAH homopolymers were also prepared.

2.3. Gel permeation chromatography

The molecular weights and molecular weight distribution of polymer were determined by gel permeation chromatography (GPC, Agilent1100), using 0.1 M $NaNO_3$ as a mobile phase with a flow rate of 0.5 ml/min. PEG was used for calibrations.

2.4. FTIR spectroscopy

FTIR spectra of samples were measured with the KBr disk using Bio-Rad FIS 135 spectrophotometer.

2.5. ^1H NMR

^1H NMR spectra of homopolymers and coploymers were recorded in D_2O using a Bruker Advance 300 MHz spectrometer.

2.6. Turbidity measurement

The absorbance of polymer solution was measured at 500 nm as a function of temperature on a TU1810 UV–vis spectrophotometer. The temperature of the water-jacketed cell holder was controlled by a Peltier circulation bath (control accuracy: ±0.1 °C). The samples in a 1 cm quartz cell were slowly heated at a rate of 0.5 °C/min, and the solution was allowed to equilibrate for 10 min at each

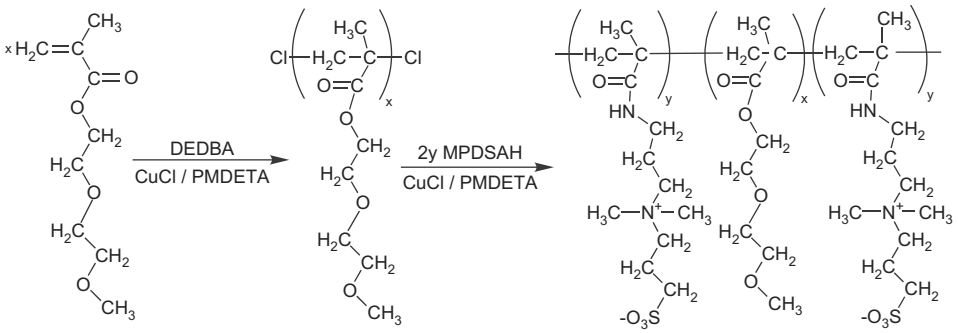

Scheme 1. Synthesis route of the $MPDSAH_y$–MEO_2MA_x–$MPDSAH_y$ block copolymers via ATRP.

temperature. Pure water was used as a reference. The temperature range was set from 1 °C to 35 °C.

2.7. Steady-state fluorescence spectroscopy

Variable temperature steady-state fluorescence spectra were recorded on an SPEX FL212 Spectrofluorometer. Temperature was controlled by a water-jacketed cell holder connected to a circulating bath. The heating rate was controlled at 0.2 °C/min, and the sample containing pyrene (1.0×10^{-7} mol/l) was equilibrated for 20 min to achieve equilibrium at each given temperature. The excitation was operated at 335 nm, and the intensities at 371 and 382 nm were used to calculate the first to third peak intensity ratio (I_1/I_3). The emission was measured between 350 and 500 nm at a scan rate of 10 nm/min. The slit openings for excitation and emission were set at 2.0 and 0.5 nm, respectively. In this study, the concentration for polymer samples is 0.1 mg/ml.

2.8. Ethidium bromide displacement assay

To confirm the binding abilities of polymers to DNA, ethidium bromide displacement assay was performed. 500 μl of polymer of desired concentrations was added into equal volumes of DNA/EB solution containing 10 μg DNA and 2.5 μg EB to obtain polymer/DNA complexes with various weight ratios. The emission intensity was measured at 590 nm (excited at 530 nm) after 15 min equilibration. The relative fluorescence intensity was expressed as the percentage of fluorescence of complexes relative to that of DNA/EB solution. The fluorescence measurements were conducted on Bio-TEK SynergyHT Microplate Reader.

2.9. AFM measurement

Polymer/plasmid DNA complexes were prepared in terms of the method described above. 5 μl of complex solution with final concentration of 1 ng/μl was deposited onto freshly split mica disks. After adsorption for 10 min, the samples were dried at room temperature for 12 h. AFM observation was conducted under ambient condition using a NanoScope IIIa atomic force microscope (Digital Instruments, Santa Babara, CA) in tapping mode at a scan speed of 1 Hz. In our case, the images of naked DNA, polymer/DNA complexes with weight ratios of 1/1, 10/1 were recorded.

3. Results and discussion

3.1. Synthesis and characterization of $PMEO_2MA$/PMPDSAH copolymers

So far, to the best of our knowledge, there were very few studies concerning ATRP of polysulfobetaine, which is possibly due to its insolubility in many organic solvents as well as the problem in realizing controlled radical polymerization [23]. In spite of these restraints, a betainic monomer, 2-methacryloyloxyethyl phosphorylcholine (MPC) was successfully polymerized in controllable manner by ATRP in aqueous and alcoholic solvents [24]. Inspired by this work, we tentatively synthesized $PMEO_2MA$/PMPDSAH copolymers in mixture of water and methanol. In view of the fact that MEO_2MA was insoluble in water, we first prepared $PMEO_2MA$ in methanol. The obtained homopolymer was aqueous soluble and used as macro-initiator to initiate copolymerization in methanol/water mixture to form ABA copolymer in which PMPDSAH and $PMEO_2MA$ were outer and inner blocks, respectively. In addition, we made PMPDSAH homopolymer in aqueous solution via ATRP. It is noted that the polydispersity index (PDI) of $PMEO_2MA$ is 1.28, but the PDIs of PMPDSAH/MEO_2MA copolymer and PMPDSAH are as broad as 2.3, indicating poor controllability of ATRP in water and water/methanol mixture, which might be resulted from hydrolytic displacement of the halogen atom or inactivation of catalyst caused by strong complexes with the transition metal ions [25]. To ensure ATRP of MPDSAH and MEO_2MA proceeds well in water system, we deliberately added sodium chloride in catalytic ingredients. From Table 1, one can see that the PDIs of PMPDSAH and PMPDSAH/MEO_2MA copolymers drop to 1.2–1.31, indicative of "controllability" with the addition of small molecular salt which was supposed to suppress the deactivator dissociation/solvolysis. It is noted that the molecular weights determined from GPC do not match NMR results. A possible reason is that our polymers contain temperature sensitive and/or polyelectrolyte segments; the aggregation of macromolecular chains even below LCST [26–28] or the association from the interaction between quaternary ammonium cations and sulfo-anions contributes to the deviation of GPC molecular weight [1].

The FTIR spectra of homopolymers display the characteristic absorption of PMPDSAH (not shown): 1642 cm^{-1} (C═O stretching), 1535 cm^{-1} (N–H bending), 1485 cm^{-1} (quaternary ammonium), 1211 cm^{-1}(S═O, asymmetric stretching) 1044 cm^{-1} (S═O symmetric stretching), and $PMEO_2MA$: 1729 cm^{-1} (C═O), 1030–1105 cm^{-1} (C–O–C) [23,29]. The feature bands of both monomers are also visible in the spectra of copolymers.

Comparing ^{1}H NMR spectra of homopolymers with that of copolymer (not shown), we find that there appear feature signals of MEO_2MA (H5: δ4.0; H2 + H3 + H4: δ3.5–3.7; H1: δ3.3; H6: δ1.8; H7: δ0.8) and MPDSAH (He: δ3.4; Hc + Hd: δ3.3; Hf: δ3.0; Hg: δ2.8; Hi: δ2.1, Hj: δ1.9; Ha: δ1.6; Hk: δ0.8) [21,30]. The results of FTIR and NMR spectra support the formation of PMPDSAH/$PMEO_2MA$ copolymers.

3.2. Double thermoresponsive behavior of copolymer in aqueous solution

Fig. 1 shows the temperature dependence of absorbance of copolymer solutions at 0.5 wt%, 1 wt%, 2 wt% and 5 wt%. Expectedly, owing to the combination of PMPDSAH and $PMEO_2MA$ in one macromolecular chain, in the course of heating, there appear UCST

Table 1
Basic data of homopolymers and copolymers.

Target block compositions[a]	Conversion of MEO_2MA[b] (%)	$\overline{M}_n$		$\overline{M}_w$	$\overline{M}_w/\overline{M}_n$[d]
		^{1}H NMR[c]	GPC[d]	GPC[d]	
MEO_2MA_{200}	65	24,468	12,270	15,770	1.28
$MPDSAH_{20}$–MEO_2MA_{160}–$MPDSAH_{20}$	56	34,561	12,650	16,570	1.31
$MPDSAH_{50}$–MEO_2MA_{100}–$MPDSAH_{50}$	53	32,740	13,710	16,860	1.23
$MPDSAH_{80}$–MEO_2MA_{40}–$MPDSAH_{80}$	50	15,907	11,750	15,040	1.28
$MPDSAH_{200}$	52	30,409	10,760	15,770	1.2

[a] Subscripts indicate the mean degrees of polymerization (DP) of each block.
[b] Conversion was determined gravimetrically.
[c] As estimated by ^{1}H NMR.
[d] Determined by GPC using 0.1 M $NaNO_3$ as eluent on the basis of PEG calibration curve.

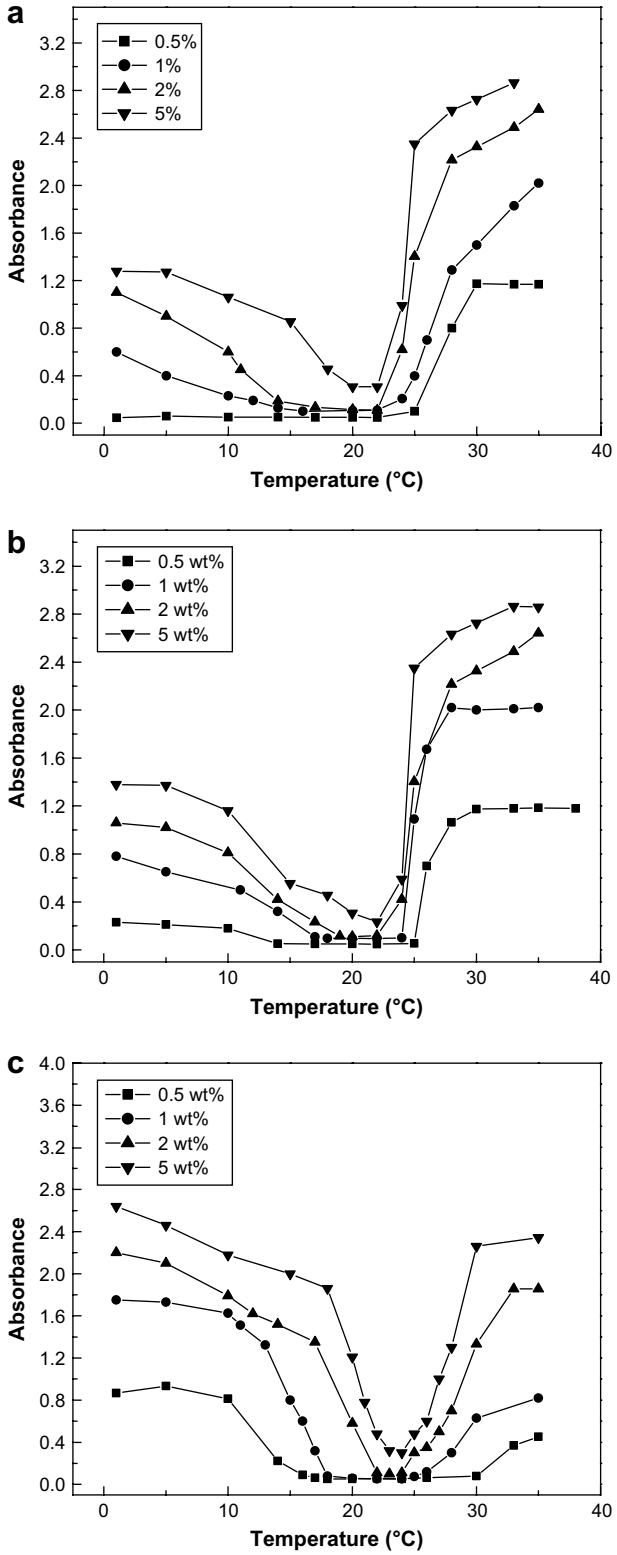

Fig. 1. Absorbance ($\lambda = 500$ nm) of polymer solutions as a function of temperature at varied concentrations. (a) $MPDSAH_{20}$–MEO_2MA_{160}–$MPDSAH_{20}$, (b) $MPDSAH_{50}$–MEO_2MA_{100}–$MPDSAH_{50}$, (c) $MPDSAH_{80}$–MEO_2MA_{40}–$MPDSAH_{80}$.

and LCST-type cloud points, which were taken at abrupt onset point (Table 2). PMPDSAH and $PMEO_2MA$ homopolymers at varied concentrations demonstrated UCST and LCST behaviors, respectively (Table 2). It should be noted that the LCSTs of $PMEO_2MA$ solutions are 4 degrees lower than those reported previously [18].

Table 2
UCST and LCST of polymer solutions with varied concentrations determined by absorbance.

Sample entry	Concentration (wt%)	0.5%	1%	2%	5%
MEO_2MA_{200}	LCST	22	22	22	22
$MPDSAH_{20}$–MEO_2MA_{160}–$MPDSAH_{20}$	UCST	–	14	16	19
	LCST	24	22	22	22
$MPDSAH_{50}$–MEO_2MA_{100}–$MPDSAH_{50}$	UCST	13	16	18	20
	LCST	25	23	22	22
$MPDSAH_{80}$–MEO_2MA_{40}–$MPDSAH_{80}$	UCST	15	18	21	23
	LCST	26	24	23	24
$MPDSAH_{200}$	UCST	16	17	20	23

The unit of temperature is degree Celsius. The error limit is ±0.1 °C.

This discrepancy may be explained from different molecular weights of polymers. Based on the relationship between Flory–Huggins interaction parameter (χ_c) and the ratio of molar volumes of polymer over solvent (r) [31]:

$$\chi_c = \frac{1}{2}\left(1 + r^{-1/2}\right)^2$$

r increases with the increment in degree of polymerization, which results in the decrease of (χ_c) Thus the polymer chains become dehydrated at lower LCST. The theoretical molecular weights of $PMEO_2MA$ obtained by us and Lutz are 24,440 and 16,900 [22], respectively. It is evident that the phase transition of our $PMEO_2MA$ occurs earlier. The similar dependence of LCST of thermoresponsive polymers on molecular weight has been reported previously [28,32].

Table 2 demonstrates that LCSTs of copolymer solutions are basically independent of concentration, except for 0.5% copolymer solution, which was found to show higher LCST. Whereas MEO_2MA_{200} homopolymer displays constant LCSTs over the whole range of selected concentrations, implying the concentration does not influence the phase transition while $PMEO_2MA$ chain is sufficiently long. Comparatively, UCST is found to rely on the concentration of aqueous solution – with an increase of concentration, UCSTs of PMPDSAH and copolymer solutions are increased. The distinction in the dependence of LCST and UCST on concentration can be explained by their respective different transition mechanisms. The temperature sensitive solubility and insolubility of polybetaine is originated from buildup and breakup of ionic pairing of opposite charges along side chains during temperature change. As the concentration is raised, the closer distance of molecular chains contributes to the formation of more ion pairings between ammonium cation and sulfo-anion. In this case, high temperature is required to disrupt the electrostatic bonding to render polymer chains soluble. In contrast, the LCST-type behavior stems from the dehydration of polymer chains in solution caused by thermally induced *breakdown* of ordering water around hydrophobic groups. Thus within a range of relative higher concentration, this dehydration occurs readily and polymer chains comes out of solution while temperature is raised to a critical point. But with further diluting solution, for example, to 0.5%, more heat energy is required to bring about the association of collapsed chains because polymer chains are separated by longer distances under this condition. Thus at dilute concentration, LCST exhibits concentration dependence. The similar results were also reported by Lutz and his coworkers [19]. They showed that LCST was increased with a decrease of concentration, but became almost constant while concentration is above 0.5%.

From Fig. 1 and Table 2, we can also find that the UCST is dependent upon the block length. For $MPDSAH_{20}$–MEO_2MA_{160}–$MPDSAH_{20}$, two shorter PMPDSAH outer blocks are separated by middle long $PMEO_2MA$ chains. As a result, only less heat energy is required to dissociate the smaller fraction of crosslinking points

stemming from fewer ionic pairings, consequently resulting in lower UCST of $MPDSAH_{20}$–MEO_2MA_{160}–$MPDSAH_{20}$ in water. Along with the increment in the block length of PMPDSAH up to 160, the UCST is almost identical to that of PMPDSAH homopolymer, suggesting longer chains of PMPDSAH in copolymer have achieved a sufficient electrostatic attractive force as its parent PMPDSAH. Likewise, except for 0.5% polymer solution, the block length of $PMEO_2MA$ has very little effect on LCSTs, which is in agreement with the reported results [19]. The higher LCSTs of $MPDSAH_{50}$–MEO_2MA_{100}–$MPDSAH_{50}$ and $MPDSAH_{80}$–MEO_2MA_{40}–$MPDSAH_{80}$ in 0.5% solution might be ascribed from the hindrance effect of PMPDSAH block on the aggregation of hydrophobic segments as well as the declining chain length of $PMEO_2MA$ in copolymers.

It is noteworthy that an interesting phenomenon can be observed in Fig. 1. Upon increasing the length of PMPDSAH, UCST is inclined to come closer to LCST. Moreover, for some copolymer, higher the concentration, smaller is the difference of UCST and LCST. It is clearly seen at 5% (Fig. 1c, Table 2), there is only 1–2 °C difference between UCST and LCST when the block lengths of PMPDSAH are 100 and 160, which renders two transition regions nearly merge together and appear sharper transition peak. The above analysis provides us a clue that the spanning range from UCST to LCST can be tuned by varying MPDSAH composition.

To trace the double temperature sensitiveness in the course of heating, we examined the variation in the micropolarity of copolymer in water using pyrene as a molecular probe [33]. Herein, we recorded the change in I_1/I_3 value of pyrene versus temperature for $MPDSAH_{50}$–MEO_2MA_{100}–$MPDSAH_{50}$ solution. As shown in Fig. 2, there appears distinct feature of I_1/I_3 corresponding to UCST and LCST regions. In the range of 2–20 °C, I_1/I_3 assumes a mild increasing trend till 17 °C with a rise of temperature. However, even at the lowest temperature selected, we did not observe an evident decrease of I_1/I_3. This can be explained from solution concentration used. In detecting the micropolarity of pyrene, the polymer concentration was set at 0.1 mg/ml. It is imagined that in such diluted cold solution, although the interaction of quaternary ammonium cations and sulfo-anions is thermodynamically favored, there are fewer opportunities for the encounter of cations and anions due to the isolated macromolecular chains. Therefore, under this condition, fewer hydrophobic microdomains are formed, leaving most of pyrene locate in hydrophilic microenvironment. By comparison, with further increase in temperature, even prior to LCST, I_1/I_3 starts to diminish, suggesting earlier dehydration of macromolecular chains. The first transition in lower temperature region was considered to be originated from modest rearrangement of coil and onset of hydrophobic aggregation, and the second stage is dominated by the breakage of ether–water bonds, which leads to pronounced chain collapse [34,35]. Approaching LCST, i.e. second stage, I_1/I_3 values drop dramatically with temperature, evidencing the formation of strong hydrophobic microdomains due to serious dehydration.

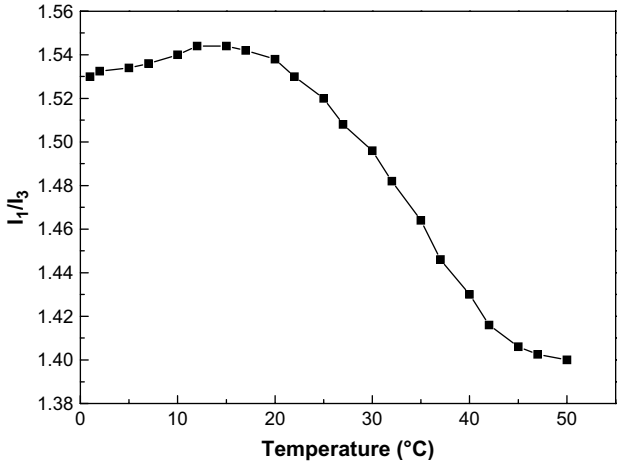

Fig. 2. Variation of I_1/I_3 versus temperature for $MPDSAH_{50}$–MEO_2MA_{100}–$MPDSAH_{50}$ solutions.

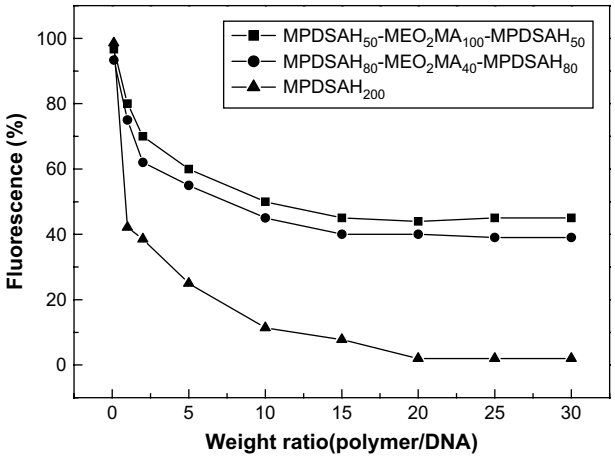

Fig. 3. Ethidium bromide displacement assay for $MPDSAH_{50}$–MEO_2MA_{100}–$MPDSAH_{50}$ (■), $MPDSAH_{80}$–MEO_2MA_{40}–$MPDSAH_{80}$ (●), $MPDSAH_{200}$ (▲).

3.3. Complexation of copolymer with DNA

Another interesting point to note from this study is DNA binding ability of PMPDSAH homopolymer as well as copolymers. Fig. 3 shows the quenching of ethidium bromide (EB) recorded for PMPDSAH/DNA and copolymer/DNA complexes. As can be observed in the figure, adding PMPDSAH to DNA/EB solution results in a salient decrease of fluorescence intensity. At low complexing ratio, 1/1, the fluorescence of EB is quenched 60%; increasing PMPDSAH/DNA ratio up to 10/1, 90% quenching effect is achieved; as complexing ratio is raised to 20/1, merely 1% fluorescence intensity is remained, that is, 99% EB is expelled out by PMPDSAH, proving its strong ability to bind DNA. That is a striking contrast to the weak capability of polycarboxybetaines to complex DNA reported by Izumrudov et al. [5,36,37]. This unexpected distinction can be interpreted from the different molecular structure of PMPDSAH and polycarboxybetaines (PCB). In PCB as shown in Scheme 2, quaternary ammonium cation is adjacent to carboxyl groups, which allows the formation of very stable ionic pair "inactivating" each other. In addition, the steric hindrance of adjacent groups and pyridine ring where cations are located further prevent DNA from approaching. Consequently, PCB displayed a poor ability to bind DNA. On the contrary, for PMPDSAH, positive and negative charges are separated by three methylene groups, which considerably lessens the spatial barrier, accordingly allowing the approachability of amino groups by external DNA, by which the 'inactive' cationic species gains 'activated state'. Therefore, DNA can be effectively complexed with PMPDSAH.

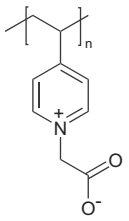

Scheme 2. Molecular structure of PCB.

We also inspected the binding affinity of copolymers with DNA. It turns out that incorporating MEO_2MA moieties weakens the binding capability of PMPDSAH to DNA. From the molecular structure and chain length, we thought there are two factors influencing the DNA binding – one is steric hindrance of $PMEO_2MA$ block, which somewhat hinders the interaction of PMPDSAH with DNA; the other is the reduction in the number of repeating unit of MPDSAH in copolymer compared to that of MPDSAH homopolymer, that is, the charge density decreases, which further lessens the capacity of copolymer to bind DNA. From Fig. 3, we can also find that $MPDSAH_{50}$–MEO_2MA_{100}–$MPDSAH_{50}$ and $MPDSAH_{80}$–MEO_2MA_{40}–$MPDSAH_{80}$ replace 54% and 60% EB, respectively. Obviously, the shorter PMPDSAH block has a lower charge density; thus at the same weight ratio of copolymer to DNA, the charge ratio of PMPDSAH block to DNA decreases, accordingly weakening the interaction with DNA, and vice versa.

The complexation of PMPDSAH and copolymer with DNA can be further confirmed by observing morphologies of DNA and complexes using atomic force microscopy (AFM). In Fig. 4, naked DNA adsorbed onto mica surface displays relaxed linear structure with partial contacts of strands, typical morphology of uncomplexed DNA [38,39]. When DNA is complexed with PMPDSAH at weight ratio 1/1, the condensates develop into nanoparticles with size of 81 nm. At higher complexing ratio, 10/1, DNA is further condensed to form more dense nanoparticles with diameter approximating to 72 nm, verifying the strong condensing capability of PMPDSAH. It is

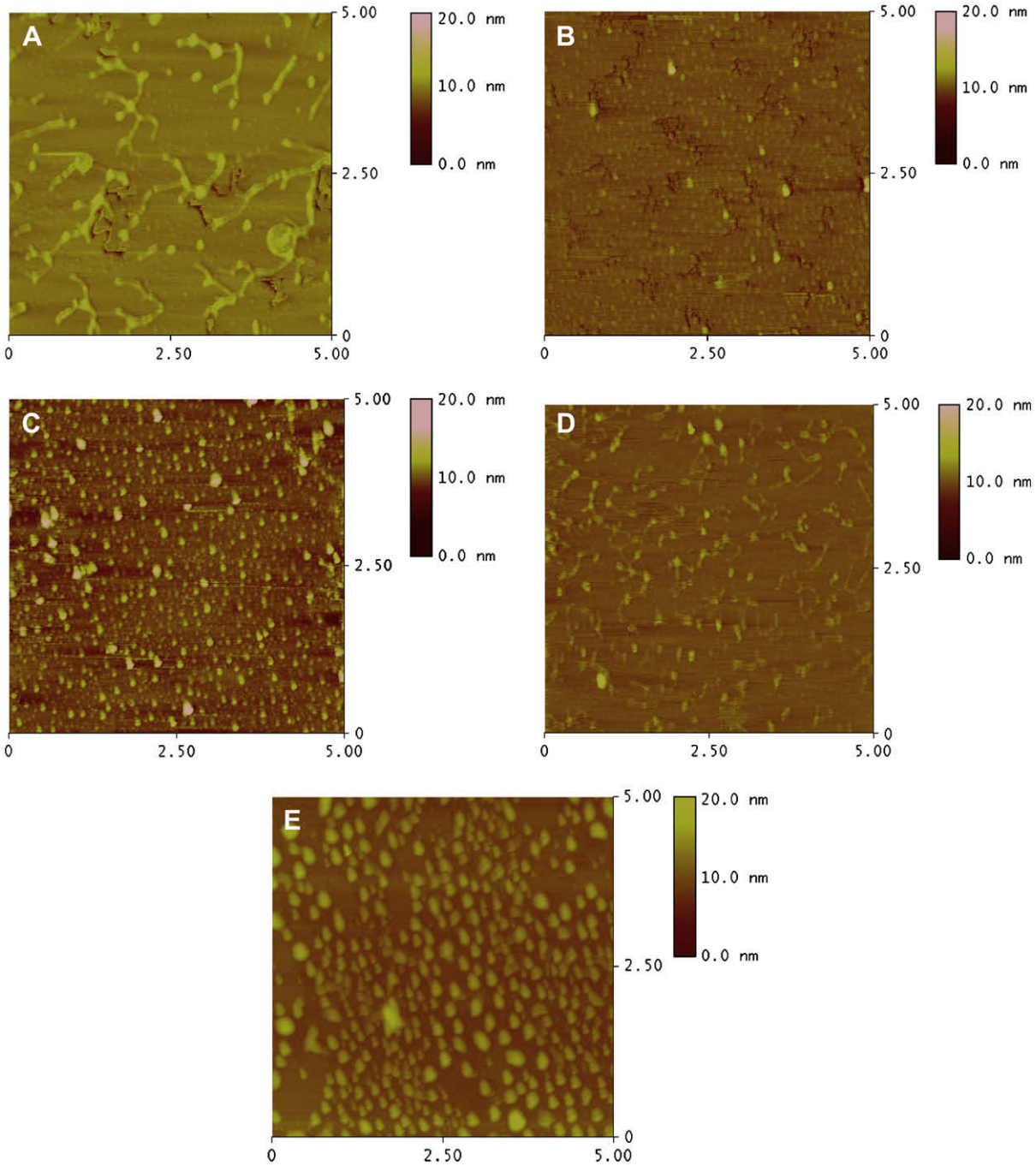

Fig. 4. AFM images (5 × 5 μm) of polymer/DNA complexes prepared at room temperature. (A) Pure DNA; (B): $MPDSAH_{200}$/DNA = 1/1; (C): $MPDSAH_{200}$/DNA = 10/1; (D): copolymer/DNA = 1/1; (E): copolymer/DNA = 10/1. Copolymer used is $MPDSAH_{50}$–MEO_2MA_{100}–$MPDSAH_{50}$.

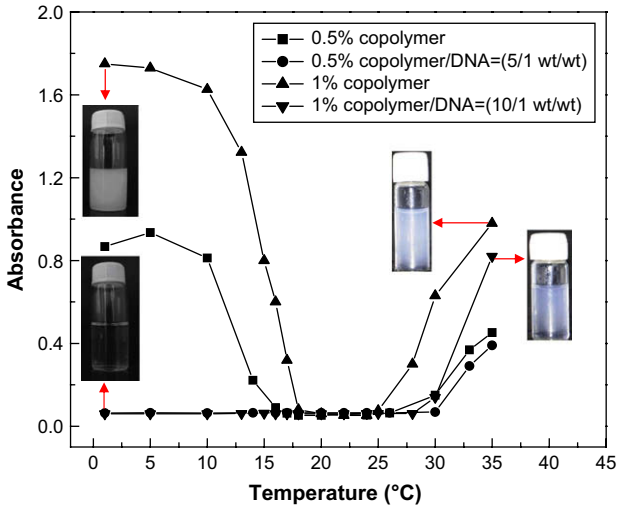

Fig. 5. Variation in the absorbance of $MPDSAH_{80}$–MEO_2MA_{40}–$MPDSAH_{80}$ solution in the absence and presence of DNA as a function of temperature. Inset shows the visual images of 1% copolymer, 1% copolymer/DNA complex taken at 1 °C and 35 °C.

easy to understand that with the increase in polymer/DNA ratio, more negative charges of DNA were neutralized to achieve more compact state, thereby resulting in smaller size of condensate particles, which is similar to the phenomenon of PEI/DNA complexes previously reported [40]. As for copolymer/DNA complexes, at ratio of 1/1, DNA molecules are not completely condensed, with tails protruding out of globular condensates, indicating poor ability to condense DNA with incorporation of MEO_2MA blocks at lower complexing ratio. Whereas copolymer/DNA complex at ratio of 10/1 demonstrates different morphology – irregular spheres are present with average size of 123 nm, and no free DNA molecules are visible, revealing an effective condensing effect. However the condensates look less compact than those formed from PMPDSAH/DNA due to suppressing effect of MEO_2MA segments in copolymer, which is consistent with the results of EB replacement.

To inspect the influence of DNA on UCST and LCST of copolymer solution, we recorded the variation in absorbance of $MPDSAH_{80}$–MEO_2MA_{40}–$MPDSAH_{80}$/DNA complex solution. Note that the selected concentrations of copolymer in solution were 0.5% and 1%, identical with that used for absorbance determination in Fig. 1 to pinpoint the influence of DNA. Fig. 5 shows that with the addition of DNA, the absorbance of solution decreases significantly and remains almost constant prior to occurrence of LCST, proving DNA binding to ammonium cations, which brings about the disruption of ion pairs and liberation of sulfonic ions in polysulbetaine chains. Thus, UCST disappears in the presence of DNA. It is visually observed that complexing DNA, copolymer solution becomes optically transparent from opacity in the absence of DNA. Nonetheless, LCSTs of 0.5% and 1% copolymer/DNA complex solutions are still existent, but increase to 29 and 26 °C, respectively. Although the turbidity is enhanced above LCST, the complex solution still remains relatively lower absorbance without whitish precipitate as occurred to copolymers in the absence of DNA (figure inset). It is evident that upon complexing DNA, surplus negative charges prevent condensates from aggregation in solution.

4. Conclusions

ATRP of MPDSAH and MEO_2MA could proceed well in water system with addition of sodium chloride into catalytic ingredients. ABA type $MPDSAH_y$-$PMEO_2MA_x$-*b*-$MPDSAH_y$ triblock copolymers obtained in this study demonstrated thermoresponsive "schizophrenic" phase transition behaviors in water due to the coexistence of UCST and LCST in one single molecule. UCST was found to rely on solution concentration, but LCST was basically independent of concentration, except for 0.5% solution. Upon increasing block length of MPDSAH and solution concentration, UCST was prone to merge together with LCST. The ion crosslinking of cation and anion did not cause evident dehydration in the course of cooling; while heating up to LCST led to serious dehydration. $MPDSAH_{200}$ exhibited a strong ability to bind DNA. Copolymers demonstrated an attenuated capability to complex DNA due to the steric hindrance of $PMEO_2MA$ block introduced as well as the decrease of charge density. Nonetheless, the copolymers were still able to condense DNA into nanoparticle at higher complexing ratios. Complexation with DNA could significantly improve the solubility of polysulfobetaine-based polymers in water, accompanied by the disappearance of UCST and slightly increased LCST.

Acknowledgement

The authors gratefully acknowledge the support for this work from the National Natural Science Foundation of China (Grants 30770587, 50573054), Tianjin Municipal Natural Science Foundation (07JCYBJC02800), and Program for New Century Excellent Talents in University.

References

[1] Berlinova IV, Dimitrov IV, Kalinova RG, Vladimirov NG. Polymer 2000;41:831.
[2] Vamvakaki M, Billingham NC, Armes SP. Polymer 1998;39:2331.
[3] Niu A, Liaw DJ, Sang HC, Wu C. Macromolecules 2000;33:3492.
[4] Kharlampieva E, Pristinski D, Sukhishvili SA. Macromolecules 2007;40:6967.
[5] Izumrudov VA, Domashenko NI, Zhiryakova MV, Rakhnyanskaya AA. Macromol Rapid Commun 2005;26:1060.
[6] Yuan JJ, Armes SP, Takabayashi Y, Prassides K, Leite CAP, Galembeck F, et al. Langmuir 2006;22:10989.
[7] Nagaya J, Uzawa H, Minoura N. Macromol Rapid Commun 1999;20:573.
[8] Zhang Z, Chao T, Chen S, Jiang S. Langmuir 2006;22:10072.
[9] Chang Y, Liao SC, Higuchi A, Ruaan RC, Chu CW, Chen WY. Langmuir 2008;24:5453.
[10] Andrew BL, Lowe AB, McCormick CL. Chem Rev 2002;102:4177.
[11] Kudaibergenov S, Jaeger W, Laschewsky A. Adv Polym Sci 2006;201:157.
[12] Mary P, Bendejacq DD, Labeau MP, Dupuis P. J Phys Chem B 2007;111:7767.
[13] Liaw DJ, Huang CC, Sang HC, Kang ET. Langmuir 1999;15:5204.
[14] Lowe AB, Billingham NC, Armes SP. Chem Commun 1996;13:1555.
[15] Chang Y, Chen SF, Zhang Z, Jiang SY. Langmuir 2006;22:2222.
[16] Arotçüaréna M, Heise B, Ishaya S, Laschewsky A. J Am Chem Soc 2002; 124:3787.
[17] Vihola H, Laukkanen A, Valtola L, Tenhu H, Hirvonen J. Biomaterials 2005; 26:3055.
[18] Han S, Hagiwara M, Ishizone T. Macromolecules 2003;36:8312.
[19] Lutz J-F, Akdemir O, Hoth A. J Am Chem Soc 2006;128:13046.
[20] Lutz J-F, Andrieu J, Uzgun S, Rudolph C, Agarwal S. Macromolecules 2007; 40:8540.
[21] Lutz J-F, Weichenhan K, Akdemir O, Hoth A. Macromolecules 2007;40:2503.
[22] Lutz J-F, Hoth A. Macromolecules 2006;39:893.
[23] Cho WK, Kong B, Choi IS. Langmuir 2007;23:5678.
[24] Ma Y, Tang Y, Billingham NC, Armes SP, Lewis AL. Biomacromolecules 2003;4:864.
[25] Tsarevsky NV, Pintauer T, Matyjaszewski K. Macromolecules 2004;37:9768.
[26] Yan JJ, Ji WX, Chen EQ, Li ZC, Liang DH. Macromolecules 2008;41:4908.
[27] Cao ZQ, Liu WG, Gao P, Yao KD, Li HX, Wang GC. Polymer 2005;46:5268.
[28] Yamamoto SI, Pietrasik J, Matyjaszewski K. J Polym Sci Part A 2008;46:194.
[29] Maeda Y, Kubota T, Yamauchi H, Nakaji T, Kitano H. Langmuir 2007;23:11259.
[30] Lee WF, Tsai CC. Polymer 1994;35:2210.
[31] Patterson D. Macromolecules 1969;2:672.
[32] Lessard DG, Ousalem M, Zhu XX. Can J Chem 2001;79:1870.
[33] Winnik FM, Ringsdorf H, Venzmer J. Langmuir 1991;7:905.
[34] Rice CV. Biomacromolecules 2006;7:2923.
[35] Zhang Y, Furyk S, Bergbreiter DE, Cremer PS. J Am Chem Soc 2005;127:14505.
[36] Izumrudov VA, Zelikin AN, Zhiryakova MV, Jaeger W, Bohrisch J. J Phys Chem B 2003;107:7982.
[37] Izumrudov VA, Domashenko NI, Zhiryakova MV, Davydova OV. J Phys Chem B 2005;109:17391.
[38] Bezanilla M, Manne S, Laney DE, Lyubchenko YL, Hansma HG. Langmuir 1995;11:655.
[39] Allen MJ, Bradbury1 EM, Balhorn R. Nucleic Acids Res 1997;25:2221.
[40] Ahn HH, Lee JH, Kim KS, Lee JY, Kim MS, Khang G, et al. Biomaterials 2008;29:2415.